Available online at www.sciencedirect.com

ScienceDirect

Physics Procedia 5 (2010) 317–326

Physics Procedia

www.elsevier.com/locate/procedia

LANE 2010

Removal of spatter by chemical etching after microdrilling with high productivity fiber laser

Ali Gökhan Demir[a]*, Barbara Previtali[a], Massimiliano Bestetti[b]

[a]*Politecnico di Milano, Dipartimento di Meccanica, Via La Masa 1, 20156 Milan, Italy*
[b]*Politecnico di Milano, Dipartimento di Chimica, Materiali e Ingegneria Chimica "G.Natta" Via Mancinelli 7, 20131 Milan, Italy*

Abstract

In this work, improved productivity in titanium microdrilling is proposed with a solution that comprises of use of a fiber laser system with nanosecond pulses and the removal of generated spatter by means of chemical etching. In particular the paper is aimed at pointing out the action exerted by the chemical solution on both the melted and heat affected zones surrounding the laser drilled hole. In the experimentation, microholes with spatter are laser microdrilled on titanium making use of a nanosecond pulsed fiber laser in the condition which minimizes the drilling time. Then spatter is chemically etched with a H_2SO_4+HF aqueous solution. The decrease in the spatter area and the change in entrance and exit hole diameters are evaluated as a function of etching time.

Keywords: Laser microdrilling; titanium; spatter removal; chemical etching; productivity

1. Introduction

The attention on generating micro scale features is increasing as the need to have better defined and detailed micro patterns grows, as well as the recent miniaturization trend proceeds both in terms of scientific research and industrial value. Very often micro scale features have to be obtained on advanced engineering materials which in return are difficult to be machined. Titanium and its alloys are a typical example of this case. The high strength/density ratio together with the low elastic modulus make titanium a suitable material for aeronautical applications, and due to its biocompatibility and high corrosion resistance for surgical, orthopaedic, dental implants, cardiac applications and hard tissue replacements [1-3]. On the other hand these advantageous properties render titanium a difficult material for processing. The high strength and low elastic modulus result in rapid tools wear, higher workpiece vibrations and spring back [4]. Its high reactivity produces chips adhesion to the tool surfaces and as a consequence premature tool breakage. Finally its low thermal conductivity promotes high temperature in the interaction area between the tool and material to be high, promoting the tool wear. Moreover, in micro range the

* Corresponding author. Tel.: +39-02-2399-8538; fax: +39-02-2399-8585.

E-mail address: ali.demir@mail.polimi.it.

1875-3892
doi:10.1016/j.phpro.2010.08.152

contribution other phenomena such as grain size and minimum chip thickness effects takes the micro chip removal processes of titanium to a more complex level [5].

Due to these limiting factors encountered in conventional machining of titanium, laser processing can be successfully adopted as an effective alternative process for titanium micromaching. Among the microfeatures that laser micromachining make feasible, to produce high aspect ratio holes is very relevant in sectors where titanium is traditionally used, such as aerospace, biomedical, food, chemical and petrochemical industries.

Laser ablation with very short pulse length enables the direct transition from solid to vapour phase [6]. Thermal conduction in the processed material can be neglected. Clean and highly precise features can be obtained, without re-casted and thermal altered layers around the hole. These well know positive advantages are counterbalanced by some drawbacks, which slows down the industrial diffusion of the ultrashort laser sources. These are the lower material removal rate, higher cost and complexity compared to the nanosecond laser sources.

On the contrary in nanosecond regime pulse lengths are long enough for the thermal wave to propagate into the processed area and melt the material. Thus the material firstly reaches the molten state and evaporation occurs from this state. Therefore microfeatures obtained by nanosecond laser sources are characterized by molten material which resolidified mainly around the hole entrance and the inner surface as well as by oxidation and heat affected zone. This is particularly evident in laser machining titanium and its alloys, due to their relatively low density and prevalent melting-contributed material removal mode [7]. Titanium has a tendency to generate a large amount of spatter during laser microdrilling. Furthermore holes drilled with a nanosecond laser are slightly tapered while circularity is scarce [7-10]. On the other hand laser systems working in nanosecond regimes can produce pulse repetition rates and pulse energy higher than the reference values obtainable in femto and pico second regime. This fact makes these laser sources the actual industrial solution when high removal rate and short process times are required. Spatter generation can be reduced through an optimized selection of laser process parameters, or to the addition of an opportune coating [8]. Also the use of novel shielding gas nozzle is proved to be suitable for this purpose [7]. However, the usual solution is to perform the mechanical or chemical removal of the spatter. Mechanical polishing, on the other hand, can result in hole closure.

Chemical etching, in the form pickling, is used widely in the industry for surface treatment of metals for scale removal and deoxidization [11,12]. The use of chemical attack to remove burr or dross in micro scale is a process widely used especially in stent manufacturing. Several authors have reported the use of acids to treat the and improve the quality of laser cut stents. [13-16]. On the contrary, to the author knowledge the consideration of chemical etching to treat laser microdrilled holes on a metal to remove spatter is scarcely explored in literature, despite the fact that it is largely applied.

This work is aims to employ chemical etching on laser microdrilled holes on titanium to remove spatter and recover the morphological integrity of the holes. The conventional use of chemical attack to remove oxidized or thermally damaged layers imply that the process is dependent on the pre-treatment of the work piece. Thus, it has been decided to define one set of laser microdrilling parameters and investigate the chemical etching in time as a function of time on laser microdrilled holes obtained using these parameters. Furthermore, for improving industrial productivity, the range of applicability and the evolution of quality characteristics of the drilled holes can be assessed properly this way.

2. Experimental design

In the following the experimentation phases are explained along with the chosen parameters. Commercially pure (cp) titanium grade 2 cold rolled sheets (thickness 450 μm) were used for the experimentations. The nominal chemical composition of the material is reported in Table 1. Test specimens were cut from the coiled material using a rotary saw machine. The specimens were polished on the edges to smoothen these surfaces and remove the burr. They were then degreased in acetone and dried in ambient air. In the following, the used setup and process parameters are explained along with the execution of the experiments.

Table 1. Nominal chemical composition of the used grade 2 commercially pure titanium [wt%]

N	C	H	Fe	O	Ti
0.005	0.006	0.002	0.04	0.156	Balance

2.1. Laser microdrilling of cp titanium

The laser microdrilling process was carried out with a 50 W IPG Photonics pulsed fiber laser system. Double clad fiber doped with ytterbium ions constitutes the active medium of this laser (λ = 1064 nm). Pumping is achieved by diode arrays. The laser source is employed with a Q-switching system that enables the system to have a pulse repetition rate in kilohertz order and generate pulse widths in nanosecond regime. The collimated diameter of the laser beam is 5.9 mm. The main variable process parameters of the laser source are pulse frequency (20-80 kHz) and pump current (10-100%). The source is equipped with LaserMech drilling head that is equipped with a 60 mm focal lens and a coaxial nozzle for shielding gas. The minimum laser spot diameter in this setup is about 23 μm. For the work piece handling Aerotech 2-axis NC table equipped with a PC interface to control the movement was used. The process parameters were fixed under the guidance of previous works [7, 8], in order to design a robust and productive process that minimizes the process time and enables to drill through holes with the presence of spatter. The laser beam was focused on top of the samples. No shielding gas was used in order to evaluate all the defects including oxidation and penetration of recast layer inside the drilled hole. Seven samples, with 10 micro holes on each were prepared. The chosen parameters are reported in Table 2. After drilling the test specimens were once again degreased in acetone. SEM images of the entrance and exit holes were acquired to reveal the morphology of the holes after drilling. Images belonging to one of these samples were chosen to represent the pre etching state (t=0 min.).

2.2. Chemical etching of the microdrilled holes

The main process variables for chemical etching are the solution type, process temperature and process time. In this part of the experimentation the solution type and process temperature were fixed and the etching duration was varied in order to investigate the evolution of spatter removal with time. For each sample 100 ml of fresh solution was used. The fixed and varied parameters for chemical etching are reported in Table 3. The samples were degreased in acetone once more prior to etching. A single laser microdrilled sample with 10 holes, which has been previously analyzed using SEM, was immersed in the acidic solution for each of the listed etching durations. Following, SEM images of the etched holes were acquired.

Table 2. Process parameters of laser micro drilling experimentation

Fixed parameters	
Pump current (%)	75
Pulse frequency (kHz)	50
Pulse width (ns)	110
Output power (W)	45
Focal position (mm)	0
Focal length (mm)	60
Beam diameter (μm)	23
Shielding gas	None
Laser emission (ms)	3

Table 3. Process parameters of chemical etching experimentation

Fixed parameters	
Solution type	Aqueous 1 M H_2SO_4 + 1 wt% HF
Solution volume	100 ml
Etching temperature (°C)	25
Varied parameter	
Etching duration (min.)	4, 8, 12, 16, 20, 24, 28

2.3. Quality assessment and measurements

SEM images were used for qualitative and quantitative analyses. According to the images the holes were grouped in order to assess a qualitative measure, the main criterion being fully etched or not. Next measurements for quantitative evaluations were carried out by means of image acquisition software. The measurements were only taken for clean hole zones, thus the entrance and exit holes that were still in the intermediate etching state were excluded from measurements due to the difficulty to define the hole. In the SEM images the measurements were taken on the surface hole. The measures taken on the clean holes were:

Mean diameter of entrance and exit holes D_{ent} and D_{ext}. Mean diameter is the average length of diameters measured at 2 degree intervals and passing through the hole centroid:

$$D = \frac{1}{180} \cdot \sum_{\theta=1}^{180} D\,(2\theta) \tag{1}$$

Taper of the holes. A perfectly cylindrical hole has a taper angle of 0°. Any difference in between two diameters results in having conical holes. Once the exit and entrance hole diameters are measured and the thickness of the material (h) is known the taper angle of the microholes can be calculated using the following formula:

$$\alpha = \tan^{-1}[(D_{ent} - D_{ext})/2h] \tag{2}$$

Aspect of entrance and exit of the holes A_{ent} and A_{ext}. Aspect is the ratio between major axis and minor axis of ellipse equivalent to the hole. The aspect of a perfectly circular hole is equal to one, on the contrary it is higher than one.

$$A = \frac{Axis_{max}}{Axis_{min}} \tag{3}$$

Adversely spatter area around the entrance $Area_{spt}$ was measured only on the holes where spatter was present.

Finally the cross sections of laser microdrilled holes before chemical etching and after chemical etching of 28 minutes were made. The optical microscope images were used to characterize the section morphologies and Vickers hardness measures were taken in order to assess the hardness along the sections. The applied load was 10 mN. The measures were taken on 3 different zones that are near the hole entrance, along the centre and along the exit. For each zone, four points were tested along the section advancing from the border to the base material.

3. Results

SEM images of the holes after laser microdrilling revealed that process is stable and reproducible. The first observations on the SEM images belonging to the etched holes suggested in a qualitative manner that etching progression was different around different micro hole zones. The evolution of etching was more rapid in case of the exit holes. The spatter area became larger initially and then gradually became smaller; suggesting a hidden molten area possibly existed around the entrance zone of the holes. Furthermore the etching occurred differently inside the holes as a detachment of an inner cone was observed in the images. Next, according to the SEM images the chemical etching was evaluated for 3 different zones that can be listed as:

1. Entrance: The dominant defect around the entrance of the holes is the spatter. The etching is considered to be completed for this zone when the whole spatter is removed.
2. Internal: The main defect inside the holes is the recast layer and the heat affected zone. SEM images revealed that chemical etching detaches a cone from the internal zone of the hole. The etching of this zone is considered to be completed once there is no semi-detached particle left inside the hole.
3. Exit: The most dominant defect around the exit of the holes is oxidation along with the accumulation of the recast layer on the bottom. The detachment of a cone layer from the hole is also evident in this case. The etching of the exit zone is considered to be complete when the zone is free of particles.

Accordingly, the etching was evaluated in two different states for these zones as being either ongoing or complete. The number of the ongoing etching zones as a function of etching duration is reported in Figure 1. It can

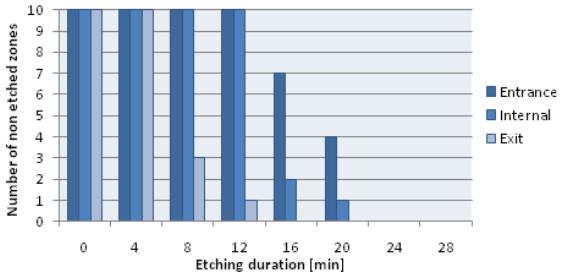

Fig. 1. The number of non etched entrance, internal and exit zones for different etching durations

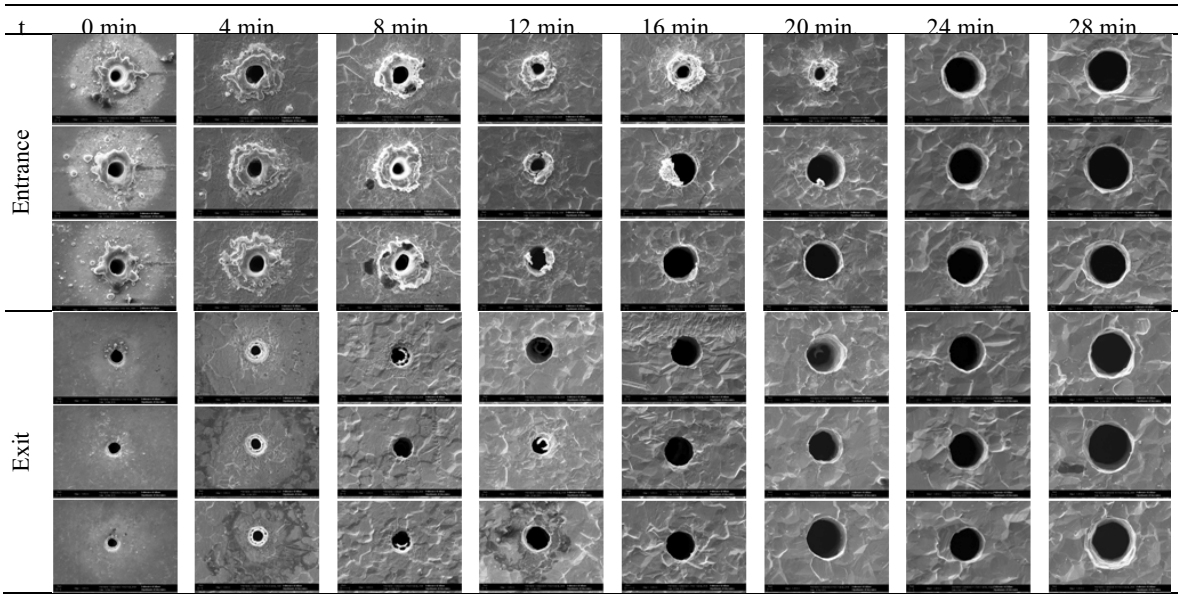

Fig. 2. Entrance and exit SEM images of laser microdrilled holes for different chemical etching durations (each image 296 μm x 222 μm)

be observed that the etching did not have any cleaning effect on any of the hole zones until 8 minutes. The cleaning effect is firstly observable for exit zones at 8 minutes, where there are only 3 holes that have non etched exit zones. The first clean internal and entrance zones were achieved at 16 minutes. This is also the point where all the exit zones were clean. The number of non clean internal zones are less than entrance zones at 16 and 20 minutes, though the etching of both zones were completed at 24 minutes. This implied that the etching speed for the entrance zone was the highest, and the lowest for entrance zone, whereas internal zone was in between the two. The hole zones were all clean after 24 minutes, expectedly further chemical attack until 28 minutes had the same effect. The two main defects, the spatter and the heat affected zones are most likely to cause the difference in the etching duration of different zones. The thermally stressed zones dissolve more rapidly in corrosive environments [17]. On the other hand spatter is generated through a very fast melting and resolidification process, which results in a microstructurally different zone with a complex surface morphology. Compared to flat surfaces, etching of such forms is expected to be more difficult, therefore the etching duration should be longer.

In Figure 2 SEM images belonging to laser microdrilled for various chemical etching durations are reported. In the images belonging to the condition prior to chemical etching (t=0 min) the morphology of as drilled microholes can be observed. In this condition spatter was present around the entrance, whereas the exit holes are free of spatter and are slightly smaller. The surface of the workpiece was covered with recast droplets on the top and the bottom surface was relatively smoother. The images belonging to the holes etched for 4 minutes imply that the etching was

in progress on all the hole zones. The spatter is larger compared to the initial state. Around the exit zone etching started detaching the initial exit hole from the base material by attacking the interfacial layer in between these two. Small droplets of recast material were less evident on the top surface and the grains started to reveal on both of the surfaces. After 8 minutes of etching the majority of the holes were cleaned around the exit zone, whereas the etching of internal and entrance zones were still not complete. For the holes that were not completely clean around the exit zone, it was possible to observe the detachment of the initial hole from the base material in the images. Consequently, the exit holes started becoming larger. Spatter became smaller and the grains were more evident compared to the previous state. At 12 minutes the etching started to decrease effectively the spatter area, as in the SEM images the detachment of this zone is visible. The spatter was in many cases not in one piece but was detached in zones. The exit zones were mostly clean and the internal zones were still to be etched. The enlargement of both the entrance and exit holes became more evident. After 16 minutes of chemical etching the process is complete for the exit zones as no defect was observed around these zones. The etching of the internal zone was complete for most of the holes even though there was spatter around the entrances which was in some cases not an external corona but was a single part leaning into the entrance area. The hole dimensions were evidently bigger than the previous case. 20 minutes of chemical etching removed all the defected zones for the majority of the hole replicas. The entrance zones were still under etching due to the existence of spatter, and due to the extension of the spatter into the hole some of the internal zones were also not fully etched. After 24 the cleaning process was complete where all the different zones were clean. The hole diameters were very large compared to the initial state as a consequence of the removal of the internal and exit zones of the holes along with the spatter. The top and bottom surfaces reflected the grain structure of the cp titanium. Finally, 28 minutes of chemical etching revealed that the cleaning effect of the process was similar to that after 24 minutes. Though, consequently the hole diameters kept enlarging.

The measurements revealed a significant change in the entrance and exit hole diameters, yet the change in aspect was rather insignificant and did not exhibit any change trend. Measurements of entrance and exit diameters and aspects were performed for the as drilled sample, which were only indicative especially in the case of entrance holes as accurate measurements are very difficult to be made for holes with spatter. In Figure 3 the initial and final hole diameters are shown along with the corresponding taper values. Initially the average value of D_{ent} was around 31µm and D_{ext} is around 25 µm. The taper values are positive and variant. After chemical etching of 28 minutes D_{ent} has an

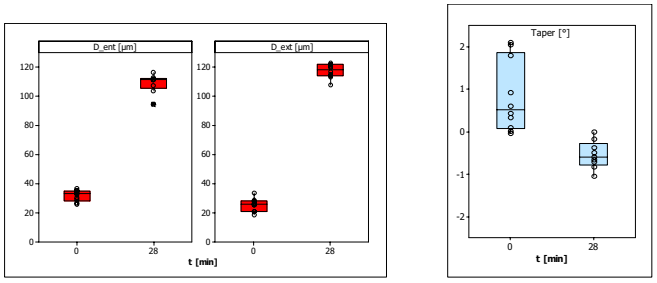

Fig. 3. Box plots of D_{ent} and D_{ext} of micro holes after laser microdrilling and after 28 minutes of etching (left) and their corresponding taper values (right)

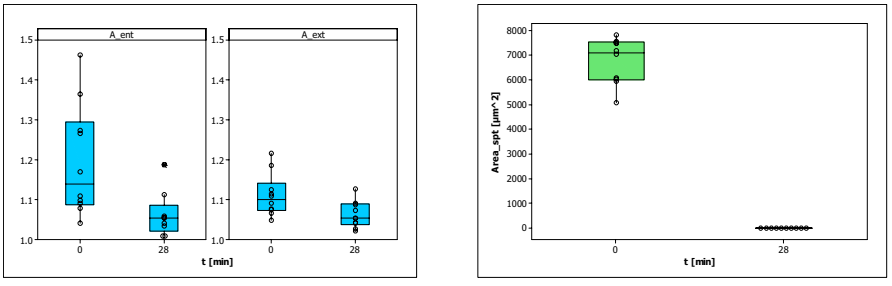

Fig. 4. Box plots of A_{ent} and A_{ext} of microholes after laser microdrilling and after 28 minutes of etching (left). Boxplots of $Area_{spt}$ of microholes after laser microdrilling and after 28 minutes of etching (right)

average value of around 108 µm and D_{ext} around 117 µm. The final taper values were negative as the exit diameters became larger than the entrance, but with smaller variance and smaller absolute values. In Figure 4 the initial and final aspect values of entrance and exit holes are reported. The values indicate that chemical etching slightly improved the circularity and reduced the variance of the values. Though, perfectly circular holes were not achieved. The initial and final values of the spatter areas are reported in Figure 4. The figure demonstrates that spatter removal was achieved at the end of the process.

Regression models were investigated for D_{ent}, D_{ext} and $Area_{spt}$ to describe the change trend of these parameters within the evolution of the process. Hole tapers and aspects were excluded from the analyses as their variance in time could not be represented with a regression model in a meaningful way. On the other hand a comparison between their initial and final values is sufficient to explain the effect of the process on these properties.

The best fit model is linear for D_{ent} and D_{ext}. In the case of D_{ent} the proposed model is:

$$D_{ent}[\mu m] = 43.1 + 2.43\ t[min] \quad (4)$$

The analysis of variance confirmed that the model in Eq.4 was adequate and the adjusted coefficient of determination R^2_{adj} was 82.5%. Lack of fit test also approved the validity of the model. Homogeneity of residuals and variance were satisfied. The main results of the regression model for D_{ent} are reported in Table 4.

Table 4. Main results of the regression model for D_{ent}.

Predictor	Coefficient	SE Coefficient	T value	P value
Constant	43.053	5.190	8.30	0.000
t	2.4329	0.2187	11.12	0.000
Regression		S = 4.41022 R^2 = 83.2% R^2_{adj} = 82.5%		

On the other hand the proposed model for D_{ext} is:

$$D_{ext}[\mu m] = 16.9 + 3.45\ t[min] \quad (5)$$

The model was confirmed by the analysis of variance and the adjusted coefficient of determination R^2_{adj} was calculated as 93.7%. The model was approved by lack of fit test. Once more homogeneity of residuals and variance were satisfied. The main results of the regression model for D_{ext} are reported in Table 5.

Table 5. Main results of the regression model for D_{ext}

Predictor	Coefficient	SE Coefficient	T value	P value
Constant	16.861	2.528	6.67	0.000
t	3.4534	0.1262	27.37	0.000
Regression		S = 5.79075 R^2 = 93.9% R^2_{adj} = 93.7%		

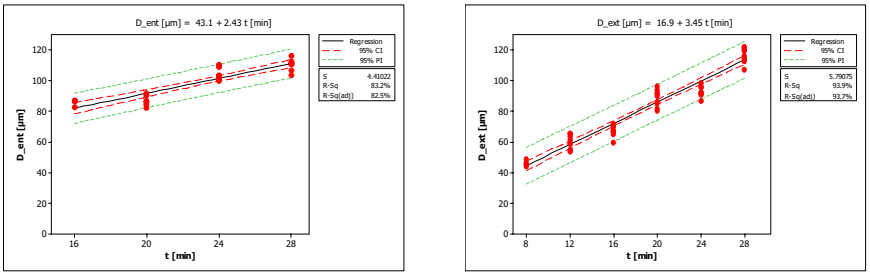

Fig. 5. Regression model and confidence intervals of D_{ent} (left) and D_{ext} (right)

The two regression models demonstrate the difference in the slopes of the fit line. The D_{ext} has a steeper slope compared to the D_{ent}. This is in agreement with the fact that at 28 minutes the taper values are negative since exit holes are bigger. This could be attributed to the fact that the existence of spatter around the entrance holes acts as a shield against the chemical attack, which prevents or eventually slows down the etching of the entrance. Using both of the models, the etching duration for obtaining entrance and exit holes with equal diameters can be estimated as 25.7 minutes, which is the intersection point of two lines. The two regression models are reported in Figure 5.

The spatter, as mentioned in the qualitative assessment, showed different behaviour in the initial phase of etching compared to the rest of the process. In the first interval of etching due to a revealing effect of the acid attack the spatter area became larger. Due to this fact the initial values of spatter areas at 0 minute were removed from the model (see Figure 6, zone 1) and the biggest spatter area values at 4 minutes were taken as the point of departure. Only holes that contained spatter for a given time instance were included in the model (see Figure 6, zone 2). The best fit model was logarithmic at the response, thus zero values at 24 and 28 minutes were also excluded (see Figure 6, zone 3). The model therefore represents the change in spatter area after the whole spatter had been revealed and for the zone where spatter is present. The proposed regression model is:

$$\ln\left(Area_{spt}[\mu m^2]\right) = 9.88 - 0.111\ t\ [min] \qquad (6)$$

In this particular model even though the normality of the residuals was satisfied, the homogeneity of variance was not fulfilled due to large dispersion of data at the final point (t=20 min), where only few holes contained spatter. In addition the model possessed an adjusted coefficient of determination R^2_{adj} equal to 74.1%. The main properties of the regression model are listed in Table 6. The scatter plot of spatter area values and the corresponding regression model are reported in Figure 6.

Table 6. Main results of the regression model for $Area_{spt}$

Predictor	Coefficient	SE Coefficient	T value	P value
Constant	9.8772	0.1194	82.73	0.000
t	-0.11133	0.01091	0.01091	0.000
Regression		S = 0.318220	R^2 = 74.8%	R^2_{adj} = 74.1%

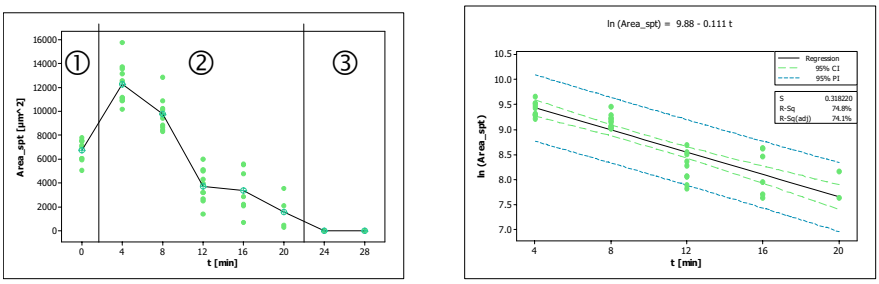

Fig. 6. Scatter plot with indicated zones and average value line to visualize the decrease (left) and regression model (right) of $Area_{spt}$

In Figure 7 images belonging to a hole section after laser microdrilling can be seen. The conicity is evident as well as some barrelling towards the exit of the hole. Furthermore the thermally altered zones are also visible especially around the entrance of the hole and along the borders. In Figure 8 the images of a hole section after 28 minutes of chemical etching are reported. The cylindricity in this case is improved and the defected zones seen in the previous case are not present anymore. Plots of the Vickers hardness measurements are reported in Figure 11. The as drilled sample hole exhibited less uniform dispersion of hardness. The increase in hardness around the entrance close to the border corresponds to the thermally altered area. On the other hand the hardness values of the section of the etched hole are more uniform, indicating the hardness value of the base material, meaning the absence of the thermally affected zone.

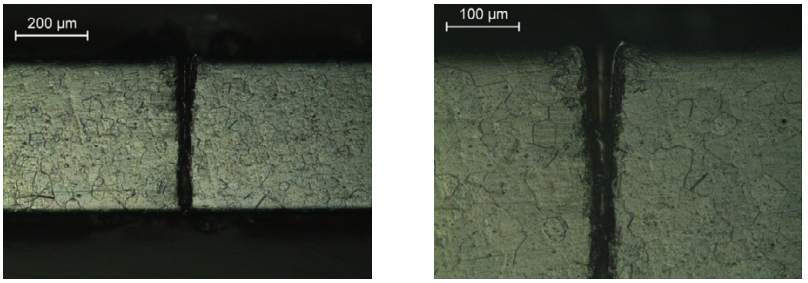

Fig. 7. Cross section of a laser microdrilled hole before chemical etching

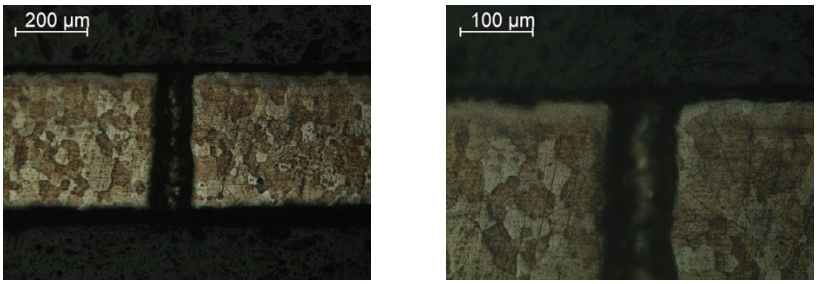

Fig. 8. Cross section of a laser microdrilled hole after 28 minutes of chemical etching

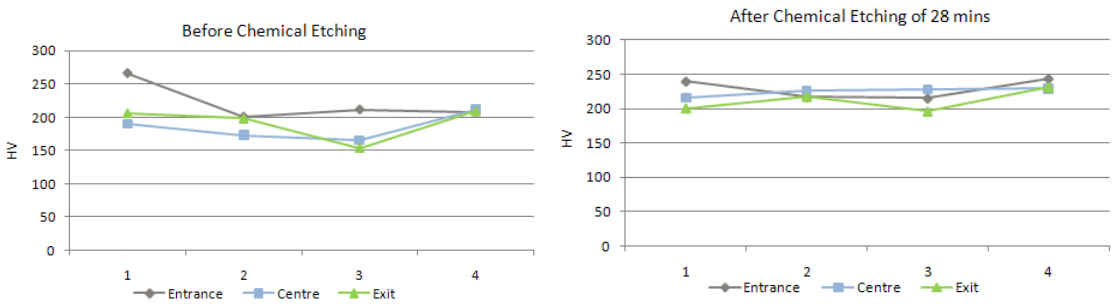

Fig. 9. Vickers hardness measurements on an as drilled hole section (left) and a hole section after 28 minutes of chemical etching

4. Conclusion

Laser microdrilling with a fiber laser system operating in nanosecond regime is a productive process, but the produced holes contain spatter that reduces the morphological quality. The other defects that are present in the drilled microholes are oxidation, conicity and recast layer inside the holes. Chemical etching of laser microcrilled cp titanium sheet with H_2SO_4+HF aqueous solution provided a solution to remove the spatter, recast layer inside the hole and oxided areas on the holes that were laser microdrilled in air with one set of parameters. Furthermore, the etching rates varied for different microhole regions, namely entrance, internal and exit. The etching was completed for the exit area first, followed by the internal zone and finally entrance. The thermally stressed zones and complex surface form of spatter were attributed to be the main reasons of different etching rates in different zones. Additionally, it was observed that between 4 and 12 minutes of chemical attack a cone-like layer was peeled from the internal and exit zones, which is believed to be the recast and heat affected layers inside the holes. The etching of all hole replicas was complete for all hole zones at 24 minutes.

Numerical measurements showed significant changes in hole diameters and spatter area values, whereas hole aspects did not exhibit a change trend throughout the process. The chemical etching enlarged hole diameters as a

compromise. Regression models for hole diameters revealed the linear increase in the values, where the exit hole diameters possessed a steeper slope, therefore a faster increase in value. Eventually, the exit hole diameters exceed entrance hole diameters and taper values became negative. The existence of spatter could have prevented effective penetration of the acidic solution on the hole profile, therefore shielded the entrance hole. On the other hand due to the absence of spatter around the exit holes, the acidic solution was not obstructed around this area, leading the exit holes to enlarge faster.

The observations and measurements put into evidence that chemical etching has a revealing effect on spatter in the initial phase. It was observed that the melted and solidified area around the entrance holes enlarged after 4 minutes of chemical etching. After this point the spatter area reduced in the time. Therefore a regression model was constructed starting from the revealed spatter dimensions until the end of etching of this area. The fit model used logarithmic transformation of the spatter area.

The cross section of non-etched holes showed the presence of thermally altered zone inside the holes as well as their form. The thermally altered zone was removed in the cross section of the etched specimen. The hardness measurements also confirmed the existence of the defected zones as the hardness varied in the non etched hole sections with an increase in the hole entrance near the border. Such variation was not observed in the etched holes.

The results of the present work confirm the effectiveness of chemical etching for the removal of spatter, but as a compromise the hole dimension change drastically. The further research should be therefore aimed at the analysis of laser process parameters along with the chemical etching variables in order to recover excessive etching of holes. The delay between the etching durations of different hole zones is one particular point to be addressed. Selection of laser process parameters to reduce spatter and mechanical polishing to weaken the spatter area prior to etching could provide the solution.

References

1. E.O. Ezugwu, J. Bonney, Y. Yamane, Journal of Material Processing Technology, 134 (2003) 233-253.
2. P.-F. Chauvy, P. Hoffmann, D. Landolt, 208-209 (2003) 165-170.
3. M. Geetha, A.K. Singh, R. Asokamani, A.K. Gogia, Progress in Materials Science 54 (2009) 397–425.
4. E.O. Ezugwu, Z.M. Wang, Journal of Material Processing Technology, 68 (1997) 262-274.
5. X. Liu, R.E. DeVor, S.G. Kapoor, K.F. Ehmann, ASME Journal of Manufacturing Science and Engineering, 126 (2004) 666-678.
6. B.N. Chicbkov, C. Momma, S. Nolte, F. von Alvensleben, A.Tünnermann, Applied Physics A, 63 (1996) 109-115.
7. C.A. Biffi, B. Previtali, Proceedings of the Fifth International WLT-Conference on Lasers in Manufacturing, (2009) 583-589.
8. C.A. Biffi, B. Previtali, Proceedings of ICALEO 2008, LIA, (2008) ICAL08_M106 27-36.
9. B.S. Yilbas, Journal of Material Processing Technology, 70 (1997) 264-273.
10. M. Ghoreishi, O.B. Nakhjavani, Journal Of Materials Processing Technology 196 (2008) 303–310.
11. R.M. Hudson, Pickling and Scaling, *ASM Handbook*, Vol. 5, Online Edition, edited by C.M. Cotell et al. ASM International, Materials Park, OH, USA, 1994.
12. A. Bloyce, P.H. Morton, T. Bell, Surface Engineering of Titanium Alloys, *ASM Handbook*, Vol. 5, Online Edition, edited by Cotell CM et al. ASM International, Materials Park, OH, USA, 1994.
13. C. Sittig, M. Textor, N.D. Spencer , M. Wieland, P.-H. Vallotton, Journal of Materials Science: Materials in Medicine, 10 (1999) 35-46.
14. H. Zhao, J. Van Humbeeck, J. Sohier, I. De Scheerder, Journal of Materials Science: Materials in Medicine, 13 (2002) 911-916.
15. Y.P. Kathuria, Journal of Materials Processing Technology, 170 (2005) 545–550.
16. H. Zhao, R. Stalmans, J. van Humbeeck , I. de Scheerder, Journal de Physique IV, 122 (2003) 2 1125-1128.
17. G.T. Burstein, L.L. Shreir; R.A. Jarman, *Corrosion,* Vol. 1, 3rd Edition, Butterworth-Heinemann, Linacre House, Oxford, UK, 1994.